Chemistry & Biology
Article

# Evolved Stereoselective Hydrolases for Broad-Spectrum G-Type Nerve Agent Detoxification

Moshe Goldsmith,[1] Yacov Ashani,[2,4] Yair Simo,[1] Moshe Ben-David,[2] Haim Leader,[3] Israel Silman,[4] Joel L. Sussman,[2] and Dan S. Tawfik[1,*]
[1]Department of Biological Chemistry
[2]Department of Structural Biology
[3]Department of Materials and Interfaces
[4]Department of Neurobiology
Weizmann Institute of Science, Rehovot 76100, Israel
*Correspondence: dan.tawfik@weizmann.ac.il
DOI 10.1016/j.chembiol.2012.01.017

## SUMMARY

**A preferred strategy for preventing nerve agents intoxication is catalytic scavenging by enzymes that hydrolyze them before they reach their targets. Using directed evolution, we simultaneously enhanced the activity of a previously described serum paraoxonase 1 (PON1) variant for hydrolysis of the toxic $S_P$ isomers of the most threatening G-type nerve agents. The evolved variants show ≤340-fold increased rates and catalytic efficiencies of 0.2-5 × $10^7$ $M^{-1}$ $min^{-1}$. Our selection for prevention of acetylcholinesterase inhibition also resulted in the complete reversion of PON1's stereospecificity, from an enantiomeric ratio (E) < 6.3 × $10^{-4}$ in favor of the $R_P$ isomer of a cyclosarin analog in wild-type PON1, to E > 2,500 for the $S_P$ isomer in an evolved variant. Given their ability to hydrolyze G-agents, these evolved variants may serve as broad-range G-agent prophylactics.**

## INTRODUCTION

G-type nerve agents—tabun (GA), sarin (GB), soman (GD) and cyclosarin (GF; Figure 1A)—are highly toxic organophosphates (OPs) that penetrate the body by both inhalation and skin absorption (Romano et al., 2008). Following their entrance, G-agents bind to and inhibit the enzyme acetylcholinesterase (AChE), thus causing a cholinergic crisis that may result in respiratory failure and death (Newmark, 2007). All G-agents possess a chiral phosphorous center, and their optical isomers differ in their toxicity. The $S_p$ isomers of GB, GD, and GF inhibit acetylcholinesterase (AChE) >1,000-fold faster than their respective $R_p$ isomers and can be >100-fold more toxic in vivo (Benschop and Dejong, 1988). GD additionally contains a chiral carbon center (Figure 1A) and is synthesized as a racemic mixture of four optical isomers. However, only its two $S_p$ isomers are considered toxic: $S_pS_c$ and $S_pR_c$ (Benschop et al., 1984). In the case of GA, nomenclature conventions ascribe an $R_p$ configuration to its toxic isomer (Carletti et al., 2010). Current treatments following OP intoxications are symptomatic and do not act to intercept the OP before it reaches its target (Cannard, 2006; Dunn and Sidell, 1989). A better treatment strategy would employ OP hydrolyzing enzymes as prophylactic drugs that would promote rapid OP degradation in vivo (Doctor and Saxena, 2005; Lenz et al., 2007). Unfortunately, all OP-hydrolyzing enzymes isolated thus far hydrolyze the toxic isomers of nerve agents with low catalytic efficiencies (diTargiani et al., 2010; Theriot and Grunden, 2011). Attempts to increase the activities of OP-hydrolyzing enzymes have been reported (for recent examples, see Hemmert et al., 2011; Tsai et al., 2010). However, currently there are no available enzymes that can hydrolyze the toxic isomers of nerve agents at sufficiently high rates to confer effective prophylactic protection using low protein doses (≤50 mg/70 kg). PON1 is a mammalian lactonase that resides in the liver and on HDL blood particles and plays a role in drug metabolism and in the prevention of atherosclerosis (Draganov, 2010; Seo and Goldschmidt-Clermont, 2009). In addition, it exhibits promiscuous OP-hydrolyzing activities (Harel et al., 2004; Khersonsky and Tawfik, 2005). Human PON1, and the other mammalian PONs, hydrolyse G-agents at low catalytic efficiencies and react primarily with their less toxic $R_p$ isomers (Amitai et al., 2006). Previously, using directed evolution, we obtained recombinant PON1 (rePON1) variants that efficiently hydrolyze the toxic $S_p$ isomer of GF (≤1.75 × $10^7$ $M^{-1}$ $min^{-1}$) and demonstrated the in vivo prophylactic activity of such an evolved variant in mice using a GF surrogate (Gupta et al., 2011). The model we had developed, and our in vivo protection experiments, indicate that the catalytic efficiency (in $k_{cat}/K_M$ terms) required for effective prophylactic protection using minimal enzyme doses (≤50 mg/70 kg) against 2 × $LD_{50}$ of G-type agents should be ≥$10^7$ $M^{-1}$ $min^{-1}$ (Gupta et al., 2011).

Here, we report additional rounds of mutagenesis and screening that improved the catalytic activities of our starting variant by 3- to 340-fold and gave PON1 variants whose catalytic efficiencies toward the toxic isomers of GD, GF, and GB are up to 5 × $10^7$ $M^{-1}$ $min^{-1}$, 3.4 × $10^7$ $M^{-1}$ $min^{-1}$, and 3.2 × $10^6$ $M^{-1}$ $min^{-1}$, respectively. The overall improvements in catalytic activities of these variants relative to wild-type PON1 ranged from 40- to 3,400-fold. Although we did not screen the

 

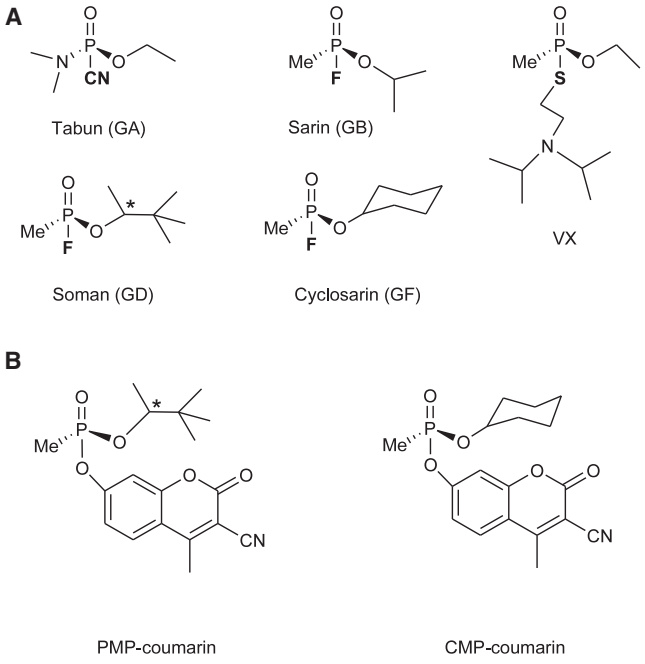


**Figure 1. Structures of the Nerve Agents and Their Analogs Used in This Work**

(A) Structures of GA, GB, GD, GF, and VX. Shown are the toxic isomers, that is, the more potent AChE inhibiting isomers ($S_P$, for GB, GD, GF, and VX; $R_p$ for GA). The chiral carbon of GD is indicated by an asterix.

(B) Structures of the $S_p$ isomers of the coumarin analogs of GD (PMP-coumarin) and GF (CMP-coumarin).

libraries with GA, the evolved variants also hydrolyze the toxic isomer of GA with catalytic efficiencies of up to 2.3 × $10^6$ $M^{-1}$ $min^{-1}$. A detailed characterization indicated that the dramatic increase in PON1's catalytic efficiency toward the toxic isomers resulted in the complete reversal of its stereospecificity from $R_p$ to $S_p$ preference. We also show that our evolved variants protect human blood cholinesterases ex vivo from inhibition by GF for at least 24 hr, thus supporting the possibility of utilizing them for in vivo prophylaxis. Finally, we found that our evolved variants had improved by >150-fold relative to wild-type PON1 for hydrolysis of the toxic isomer of VX (Figure 1A), thus providing a starting point for the directed evolution of PON1 for neutralization of V-type agents.

## RESULTS

### The Starting Point

As a starting point for directed evolution toward GD and GB hydrolysis, we used PON1 variants that were previously evolved toward GF hydrolysis (Gupta et al., 2011). These were derived from a recombinant variant of mammalian PON1, dubbed rePON1-G3C9, that is expressed functional and soluble in *E. coli* and exhibits enzymatic specificities that are essentially identical to human PON1 (Aharoni et al., 2004). The catalytic activities of the rePON1 variants that were evolved toward GF were tested with GB and GD. We found several variants that were similar in sequence and were improved relative to the wild-type-like rePON1 by up to 135- and 37-fold with the two toxic isomers of GD and up to 4-fold with the toxic isomer of GB (Table S1 available online). One of these variants, 2D8, which carried the smallest number of mutations yet exhibited the highest activity, was chosen as the starting point for further evolution (Table 1).

### Library Design and Screening

We generated gene libraries derived from 2D8 by structure-guided targeted mutagenesis. This enabled us to generate smaller and more focused libraries that could be screened by our medium-throughput 96-well plate screen. Several strategies were applied as detailed below.

#### *Strategy 1: Targeted Diversification of Active-Site Residues*

An examination of the structures of unbound PON1 (Protein Data Bank [PDB] code 1V04; Harel et al., 2004), PON1 in complex with the inhibitor 2-hydroxyquinone (PDB code 3SRG; Ben-David et al., 2012), and a docking model of PON1 with the OP pesticide paraoxon (Ben-David et al., 2012) indicated that active-site positions 70, 71, 196, 240, and 292 (Table 2) could affect OP binding and catalysis. In addition we decided to explore positions 69, 115, and 134 of active-site residues that were substituted in the earlier rounds of directed evolution toward GF hydrolysis. We constructed a library of variants by spiking mutations in these eight active-site positions into the 2D8 gene in a combinatorial manner using the ISOR method (Herman and Tawfik, 2007). In general, residues were mutated to amino acids with similar physicochemical properties, although more drastic changes were also included (e.g., Gly69Leu/Val/Ile). Sequencing of randomly selected clones revealed that the unselected library contained on average 4 ± 1 mutations per clone, with each clone exhibiting a different mutational composition. This round 1 library was then screened with in-situ-generated GD and GB, using the AChE inhibition assay (Experimental Procedures). This assay measures the ability of PON1 variants to protect AChE activity by rapidly hydrolyzing the toxic isomer of the added OP.

By the end of Round 1, all improved variants had acquired mutations at two positions, 69 and 115, which were previously mutated to improve GF hydrolysis (Gupta et al., 2011). The improved variants carried additional mutations, primarily at positions 70, 71, 196, 240, or 292, but these varied from one variant to another (Table S2).

The changes in residues 69 and 115 led us to explore the re-optimization of another key active-site residue, 222, the mutagenesis of which to Ser had led to increased GF hydrolysis (Gupta et al., 2011). We therefore explored mutations of Ser222 to hydrophobic residues (Leu, Val, Ile, Met, or Cys) in the second round (Table 2). Indeed, 96% (24/25) of the improved variant from round 2 were mutated in position 222, mostly to Met (17/24).

Positions 69, 115, and 222 that were substituted in the first two rounds reside at the bottom of PON1's active-site and close to the catalytic calcium. However, in the third round library, we targeted residues whose side chains are involved in structuring the top of PON1's active-site cleft. These included positions 50, 197, 291, 294, 346, 347, and 348. In addition, we retargeted positions 196 and 292 (Table 2). On average, variants in the unselected third round library contained 2 ± 1 substitutions at the targeted positions. Following screening with GB and GD,

**Table 1. Catalytic Activities of the Best Variant from Each Round**

| Variant | Mutations Relative to rePON1[a] | Round | Catalytic Efficiency[b] ($k_{cat}/K_M$) × $10^7$ $M^{-1}min^{-1}$ | | | | |
|---|---|---|---|---|---|---|---|
| | | | GD Fast[c] | GD Slow[c] | GF | GB | GA |
| rePON1 | – | – | 0.0055 ± 0.002 | 0.0015 ± 0.0006 | 0.013[d] ± 0.003 | 0.008 ± 0.001 | 0.043 ± 0.007 |
| 2D8 | Leu69Gly, His115Trp, His134Arg, Phe222Ser, Thr332Ser | 0 | 0.4 ± 0.1 | 0.015 ± 0.003 | 0.46[d] ± 0.01 | 0.025 ± 0.002 | 0.082 ± 0.005 |
| Fold improvement relative to (rePON1)[e] | | | (73) | (10) | (35) | (3) | (2) |
| PG11 | **Leu69Val, His115Ala**, His134Arg, Phe222Ser, Thr332Ser | 1 | 1.43 ± 0.3 | 0.32 ± 0.04 | 0.2 ± 0.03 | 0.02 ± 0.005 | 0.006 ± 0.001 |
| Fold improvement relative to variant 2D8 (rePON1)[e] | | | 4 (260) | 21 (213) | 0.4 (15) | 0.8 (3) | 0.07(0.1) |
| VII-D11 | Leu69Val, His115Ala, His134Arg, **Phe222Met, Asp309Gly,** Thr332Ser | 2 | 2.9 ± 0.9 | 2.9 ± 0.1 | 1.07 ± 0.08 | 0.12 ± 0.01 | 0.025 ± 0.003 |
| Fold improvement relative to variant 2D8 (rePON1)[e] | | | 7(527) | 193(1933) | 2(82) | 5(15) | 0.3(0.6) |
| 1-I-F11 | **Leu55Met,** Leu69Val, His115Ala, His134Arg, Phe222Met, **Ile291Leu,** Thr322Ser | 3 | 4.4 ± 0.6 | 4.4 ± 0.6 | 1.52 ± 0.1 | 0.39 ± 0.04 | 0.17 ± 0.04 |
| Fold improvement relative to variant 2D8 (rePON1)[e] | | | 11(800) | 293(2933) | 3(117) | 16(49) | 2(4) |
| IIG1[f] | Leu55Ile, Leu69Val, His115Ala, His134Arg, **Asp136Gln,** Phe222Met, Ile291Leu, Thr332Ser | 4 | 5.1 ± 0.6 | 5.1 ± 0.6 | 3.4 ± 0.3 | 0.32 ± 0.01 | 0.23 ± 0.004 |
| Fold improvement relative to variant 2D8 (rePON1)[e] | | | 13(927) | 340(3400) | 7(262) | 13(40) | 3(5) |

[a]Mutations relative to the wild-type-like rePON1 variant G3C9 (Harel et al., 2004). Mutations that were newly introduced in a given round are denoted in bold.
[b]Kinetic parameters relate to the toxic $S_p$ isomers of GB, GD and GF or to the toxic $R_p$ isomer of GA. Error ranges were derived from at least two independent measurements. The maximal deviation between different enzyme preparations was ≤2-fold.
[c]Fast and slow hydrolysis of the two equally toxic isomers of GD ($S_cS_p$ and $R_cS_p$).
[d]Values from (Gupta et al., 2011).
[e]Fold improvement in catalytic efficiencies relative to the starting variant 2D8 or relative to wild-type-like rePON1 (numbers in brackets). PG11, best variant of round 1; VII-D11, best variant of round 2; 1-I-F11, best variant of round 3; IIG1, best variant of round 4.
[f]See also Figure S5.

we obtained 18 improved clones in which positions 197 and 291 were primarily mutated (in 4/18 and 8/18 of the improved variants, respectively). Some positions did not accept any mutations (196, 294, 346, 347, and 348), and others were mutated in single clones (50 and 292).

### *Strategy 2: Shuffling of Improved Variants*

Shuffling of selected variants can combine beneficial mutations that were acquired in separate variants and/or eliminate deleterious mutations from individual variants. In particular, since the theoretical mutational diversity in our libraries was large compared to the number of clones screened (0.04% to 7% of the theoretical library diversity), the improved variants generally exhibited different mutational compositions (e.g., round three in which little convergence was seen). In effect, shuffling of improved variants was applied in every round as part of the ISOR protocol (Herman and Tawfik, 2007) that was used to introduce the library mutations. However, for the round 4 library, shuffling was applied with no spiking of targeted mutations (Table 2).

### *Strategy 3: Targeted Mutagenesis of the Flexible Active-Site Loop*

PON1's longest active-site loop (residues 70–78) is highly flexible and disordered in the crystal structures of unbound PON1 (Harel et al., 2004). Upon binding of the lactam inhibitor 2-hydroxyquinoline (2HQ), the loop became structured and thereby completed the active site (Ben-David et al., 2012). Therefore, we designed a second round 3 library that explored active-site loop mutations. Given the very small size of the fluoride

leaving-group of G-agents, we explored loop mutations that introduced large side chains, such as Trp, Phe, and Tyr, which could reduce the active site's volume and improve substrate binding. We also attempted to modulate the loop's configuration by exploring mutations to Gly and Pro (Table 2). Each clone in the unselected library carried, on average, one loop mutation.

***Strategy 4: Ancestral Mutations***

Ancestral mutations, that is, substitutions into residues that appeared along the evolutionary history of a given protein, have been shown to be powerful modulators of a protein's stability and function (Bershtein et al., 2008; Chen et al., 2010). A library based on active-site substitutions from the predicted ancestors of mammalian PONs has been described (Alcolombri et al., 2011). Screening this library with a coumarin analog of GF (CMP-coumarin; Figure 1B) led to the identification of several ancestral mutations that increase this activity (Alcolombri et al., 2011). We included these mutations (Leu55Ile, Ile74Leu, Asp136His, and Pro189Gly) together with similar ones (55Met/Val, 136Gln, and 189Ser) in the round 3 substitution library at an average frequency of 0.5 mutations per gene in the unselected library (Table 2).

## Directed Evolution of rePON1 for G-Agent Hydrolysis

Table 1 summarizes the results of four rounds of directed evolution starting from variant 2D8 and screening for GB and GD hydrolysis. After screening ~2,000 variants in round 1, we identified 21 clones that in crude cell lysates were improved up to 4-fold with GB and up to 5-fold with GD relative to the starting point 2D8 (Table S2). The two most active variants with GD, 5H8 and PG11, were purified and characterized (Tables 1 and S1). We found an improvement of 21- and 4-fold in the catalytic activity of the best variant PG11 with the two toxic isomers of GD relative to the starting variant 2D8 (Table 1). However, PG11's activity with GF was reduced 2.3-fold, and its GB activity was the same as 2D8's. The best two variants shared the same four active-site mutations—Leu69Val, His134Arg, Phe222Ser, and Thr332Ser—but differed in position 115.

For the second round, we constructed a substitution library that explored various substitutions at position 222 while shuffling the ten most active clones found in round 1 (Table S3). The resulting library was screened for GD and GB, as well as GF. The latter was included to eliminate variants that exhibit reduced activity with GF as observed with variants isolated from the first round. Of the ~1,000 clones screened, we isolated 39 improved variants, 25 of which were unique (Table S4). Following additional screens, we identified the six most active variants, purified them, and characterized them. The purified variants exhibited up to 7- and 193-fold higher specific activities with the two toxic isomers of GD and up to 5-fold higher activities with GB, relative to the starting variant 2D8 (Tables 1 and S1). Their activities with GF became similar to that of 2D8, and all but one contained a Phe222Met mutation (Tables 1 and S1). Though no attempt was made to introduce random mutations during library construction, the polymerase chain reaction (PCR) methodologies applied for library making, produced random mutations, such as Phe64Leu or Asp309Gly, which were retained in certain improved variants. By round 2, the most improved variants reached the targeted catalytic efficiency of $\geq 10^7$ $M^{-1}$ $min^{-1}$ with GD and GF but were still 10-fold lower in activity with GB. The best round 2 variant, VII-D11, hydrolyzed the two toxic isomers of GD with equally high rates ($2.9 \times 10^7$ $M^{-1}$ $min^{-1}$; Table 1).

In the third round, two libraries were constructed, and 400 variants from each library were screened with GD and GB (Tables 2 and S5). We identified 18 improved clones altogether. All these clones were improved with GB, but only 67% (12/18) were also improved with GD (Table S6). Most of the improved variants originated from library #3.1 (73%, 13/18), and their improvements with GB (1.6- to 4-fold) were greater than with GD (1.1- to 1.6-fold). Sequencing indicated that 55% (10/18) of these improved variants contained at least one ancestral mutation (Leu55Ile or Asp136His), and 28% (5/18) contained two ancestral mutations. In addition, the active-site mutation Ile291Leu became abundant (39%, 7/18). Certain mutations introduced in earlier rounds, His134Arg and Phe222Met, were fixed (i.e., appeared in all improved variants) and others, Leu69Val and His115Ala, were nearly fixed (90%, 16/18; Table S6).

We purified and characterized the four most improved variants of round 3. Relative to 2D8, their catalytic efficiencies were improved up to 11- and 293-fold with the two toxic isomers of GD and up to 17-fold with GB (Tables 1 and S1). Although 2D8 was evolved for GF, a further $\leq$3-fold improvement with GF was identified in round 3 variants. The catalytic efficiency of our most improved variant with GB (1-I-F11, $3.9 \times 10^6$ $M^{-1}$ $min^{-1}$) was improved >3-fold relative to the best round 2 variant but was still 2.5-fold lower than our goal.

In round 4 (Tables 2 and S7), 700 clones were screened with GB and GD, and 22 improved variants were isolated, of which 18 were singular (Table S8). Of these, 66% (12/18) were improved mostly with GB, and 33% (6/18) were improved also with GD. In addition to the mutations fixed in earlier rounds, His115Ala was fixed, and most variants also carried Leu55Ile (55%, 10/18) and/or Ile291Leu (83%, 15/18; Table S8). We purified nine variants and identified three variants that had improved relative to the starting variant 2D8 by $\leq$13- and 340-fold with the toxic isomers of GD, $\leq$7-fold with GB, and $\leq$9-fold with GF (Tables 1 and S1). Although their catalytic efficiencies with GB ($1.7\text{-}3.2 \times 10^6$ $M^{-1}min^{-1}$) were 3- to 6-fold lower than our desired goal, their catalytic efficiencies with GF and GD were well over $10^7$ $M^{-1}$ $min^{-1}$ (Tables 1 and S1; Figure 2).

## Neutralization of GA

The in vivo toxicity of GA is >2-fold lower than that of all other G-agents (Benschop and Dejong, 1988), thus ranking it as the least toxic of the G-agents. In addition, its structure and leaving group are significantly different than that of all other G-agents (Figure 1A), suggesting that variants improved at hydrolyzing the three other G-agents might exhibit lower rates with GA and vice versa. Thus, we did not screen our libraries for GA neutralization. Instead, we examined the activity of wild-type like rePON1 and of the most improved variants from the four rounds of evolution described here with GA. Using the AChE inhibition assay, we found that rePON1 is $\leq$40-fold more efficient at hydrolyzing the toxic isomer of GA than the toxic isomers of all other G-agents (Table 1). The most improved variants from rounds 3 and 4 became 4- to 5-fold more efficient than rePON1 at hydrolyzing the toxic isomer of GA (1-I-F11 and IIG1; Table 1). Thus, although GA neutralization was not

**Table 2. Summary of Directed Evolution Rounds**

| Round | Mutagenesis Strategy | Spiked Mutations[a] | Shuffling | Screening/ Substrate | Fold Improvement Measured in Crude Cell Lysates |
|---|---|---|---|---|---|
| 1 | 1 | Gly69Leu/Val/Ile/Ser<br>Lys70Ala/Ser/Gln/Asn<br>Tyr71Phe/Cyc/Ala/Leu/Ile<br>Trp115Leu/Cyc/Gly/Ala/Val<br>Arg134His/Gln/Asn<br>Met196Leu/Ile/Phe<br>Leu240Ile/Val<br>Phe292Ser/Val/Leu | – | 2,000 clones screened with GB,GD | 21 improved variants[b]. ≤4-fold with GB and ≤5-fold with GD relative to the starting point (2D8). Best variant: PG11 |
| 2 | 1 | Ser222Leu/Val/Ile/Met/Cys | 10 best clones from round 1[c] | 1,000 clones screened with GB, GD, and GF | 25 improved variants[d]. ≤4-fold with GB, ≤ 2-fold with GD and ≤4 fold with GF relative to PG11. Best variant: VIID11. |
| 3 | 1 | Library 3.1<br>Asn50Gly/Ala<br>Met196Phe/Ile<br>His197Lys/Ser/Arg/Gln/Asn/Thr<br>Ile291Phe/Trp/Leu<br>Phe292Leu/Ile/Trp<br>Tyr294Phe/Gln/Asn<br>Val346Leu/Ile/Phe/Trp<br>Phe347Gly/Ala/Ile/Leu/Val/Thr<br>/Ser/Trp<br>His348Gly/Ala/Ile/Leu/Val/Thr<br>/Ser/Trp | 7 best clones from round 2[e] | 400 clones from library 3.1 screened with GB and GD | 18 improved variants[f]. ≤4 fold with GB, ≤1.6-fold with GD relative to VIID11. Best variant: 1-I-F11 |
| 3 | 4 | Library 3.1:<br>Leu55Ile/Met/Val<br>Ile74Leu<br>Asp136His/Gln<br>Pro189Gly/ Ser | | | |
| 3 | 3 | Library 3.2:<br>Gly69Met/Ala<br>Lys70Ser/Gln/Thr/Glu/Asp/Arg<br>Tyr71Phe/Trp/Met/Cyc<br>Pro72Gly/Ser<br>Gly73Pro/Ser<br>Ile74Trp/Phe/Pro/Ser/Gly<br>Met75Leu/Trp/Phe/Pro<br>Phe77Gly/Ala/Ile/Leu/Val/Thr/<br>Ser/Trp/Ile/Leu/Met<br>Asp78/Asn/Gln/Ser/Ala/Val/<br>Tyr/Gly/Ser/Pro | 7 best clones from round 2[e] | 400 clones from library 3.2 screened with GB and GD | |
| 4 | 2 | No mutations spiked | 18 best variants from round 3[g] libraries 3.1 and 3.2 | 700 clones screened with GB and GD | 18 improved variants[h]. ≤2 fold with GB, ≤2-fold with GD relative to 1-I-F11. Best variant: IIG1 |

See also Figure S4.

[a]The average frequency of random mutations in unselected library clones was 0.5 ± 0.3.

[b]See Table S2.

[c]See Table S3.

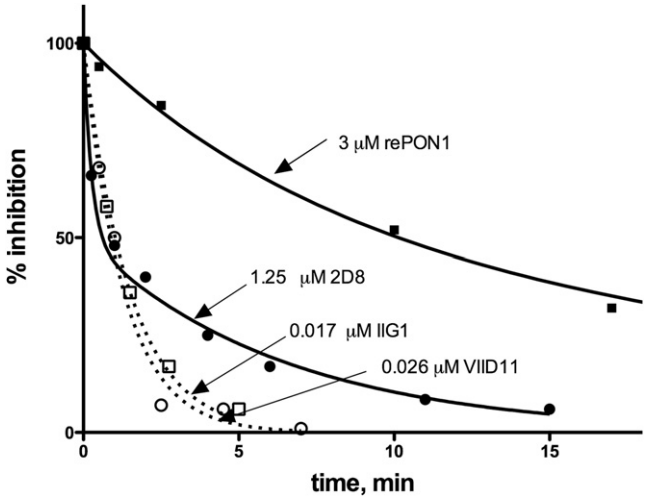


**Figure 2. Hydrolysis of GD by Evolved Variants**

Residual AChE activity was assayed and plotted as % inhibition of AChE after the incubation of in situ generated GD with variants as follows: 2D8 and VIID11 (100 nM, GD), IIG1 (80 nM, GD), and rePON1 (50 nM, GD). Variant concentrations are noted in the figure. Data were fitted to a biphasic rate equation to derive the apparent rate constants for hydrolysis of the two toxic isomers of GD.

screened for, the catalytic efficiency of our evolved variants with GA had increased and became similar to that with GB ($\sim 3 \times 10^6$ $M^{-1}$ $min^{-1}$).

## Stereospecificity of the Evolved Variants

Library screening and variant characterization were done using racemic G-agent solutions. However, the AChE assay we employed can only detect the hydrolysis of the toxic isomers of G-agents ($S_p$ for GB, GD, and GF and assuming $R_p$ for GA). To examine the hydrolysis of both stereoisomers, we assayed the most improved variants from each round of directed evolution with the purified $R_p$ and $S_p$ isomers of the coumarin analogs of GF and GD (CMP-coumarin, PMP-coumarin; Figure 1B). The activities of OP-hydrolyzing enzymes with coumarin analogs and with the G-type nerve agents themselves appear to be well correlated, not only for our engineered PON1 variants (Gupta et al., 2011) but also for other OP-hydrolyzing enzymes (Tsai et al., 2010). Our results indicated that the evolution of higher detoxification rates of the three target G-agents (GB, GD, and GF) was accompanied by a complete reversion in rePON1's stereoselectivity (Table 3). The catalytic efficiency ($k_{cat}/K_M$) of the wild-type-like rePON1 with $R_p$-CMP-coumain is >1,600-fold higher than with $S_p$-CMP-coumarin. In contrast, the $k_{cat}/K_M$ value of the best variant from round 3 (1-I-F11) with $S_p$-CMP-coumarin is >2,500-fold higher than with $R_p$-CMP-coumarin (Table 3; Figure S1).

The increase in $S_p/R_p$ stereoselectivity with CMP-coumarin was attributed to a decrease in the $K_M$ value for $S_p$-CMP-coumarin and a concomitant increase in $k_{cat}$. Parallel increases in $K_M$ and decreases in $k_{cat}$ values were observed with $R_p$-CMP-coumarin (Table 3).

A similar trend was observed with the coumarin analog of GD, PMP-coumarin (Figure 3). While the best round 1 variant hydrolyzed all four diasteroisomers of PMP-coumarin at measurable rates, variants from rounds 2 to 4 hydrolyzed only 50% of the racemic mixture (Figure 3A). To confirm that the hydrolyzed fraction corresponds to the $S_p$ isomer pair, we applied the evolved rePON1 variant 3B3 that hydrolyzes almost exclusively the $R_p$ isomers of coumarin G-agent analogs (Ashani et al., 2010). Indeed, following the action of 3B3 that hydrolyzed 50% of a racemic mixture of PMP-coumarin, the remaining 50% were readily hydrolyzed by evolved variants from rounds 2–4 (Figure 3B).

To examine the stereopreference of variants toward GA, we compared the hydrolysis rates obtained by the AChE assay that detects only the hydrolysis of the toxic isomer of GA (Table 1), to $^{31}$P-nuclear magnetic resonance (NMR) kinetics that monitored the hydrolysis of both GA enantiomers (Figure S2). The results indicated that wild-type-like rePON1 and variant 2D8 hydrolyze the toxic $R_p$ isomer of GA with similar efficiencies, $4.3 \times 10^5$ and $8.2 \times 10^5$ $M^{-1}$ $min^{-1}$, respectively, whereas variant VIID2 had improved with the toxic $R_p$ isomer ($1.83 \times 10^6$ $M^{-1}$ $min^{-1}$).

## Activity and Stability in Human Blood Samples

The use of evolved PON1 variants as prophylactic drugs depends on their ability to maintain activity in human blood over long periods of time. Previously, we showed that evolved variants 4E9 and VIID2 protect human blood cholinesterases (ChE) from inhibition by GF in an ex vivo assay (Ashani et al., 2011). Whereas this assay does not necessarily reflect their in vivo bioavailability, it comprises a facile way of assessing the stability and activity of the evolved PON1 variants in the blood. Variants PG11, VIID11, 1-I-F11, and VIID2 (from rounds 1–4, respectively) were added to human blood samples and incubated at 37°C. In-situ-generated GF was added at different time intervals, and the residual blood ChE activity was measured (Figure 4A). Becauase of its low catalytic efficiency, round 1 variant PG11 could not provide measurable ChE protection at the concentration range used (0.5–2.1 μM). However, variants VIID11, 1-I-F11, and VIID2 showed measurable ChE protection (41%–45%) after 5 min of incubation. Further, these variants maintained 80%–95% of their initial protection activity in human blood after 24 hr of incubation at 37°C (Figure 4A). The rate of CMP-coumarin hydrolysis at different time intervals following incubation in whole blood (Figure 4B) or buffer (Figure S3) also gave very similar results. Taken together, these results suggest that the interaction of the evolved PON1 variants with human

[d]See Table S4.
[e]See Table S5.
[f]See Table S6.
[g]See Table S7.
[h]See Table S8.

**Table 3. Stereoselectivity with $S_p$- and $R_p$-CMP-Coumarin**

| | | $S_P$-CMP-Coumarin | | | $R_P$-CMP-Coumarin | | | |
|---|---|---|---|---|---|---|---|---|
| Round No. | Variant | $k_{cat}$ ($min^{-1}$) | $K_M$ ($\mu M$) | $k_{cat}/K_M$ ($\mu M^{-1}$ $min^{-1}$) | $k_{cat}$ ($min^{-1}$) | $K_M$ ($\mu M$) | $k_{cat}/K_M$ ($\mu M^{-1}$ $min^{-1}$) | E ($S_p/R_p$)[a] |
| – | rePON1 wild-type-like[b] | nd[c] | nd[c] | <0.0002 | 14.5 (±0.5) | 45 (±6) | 0.322 | <0.0006 |
| 1 | PG11 | 632 (±5) | 104 (±12) | 6.1 | 106 (±2.5) | 437 (±34) | 0.243 | 25 |
| 2 | VIID11 | 500 (±19) | 105 (±1) | 4.8 | 107.5 (±4) | 1,307 (±155) | 0.082 | 59 |
| 3 | 1-1-F11 | 1004 (±98) | 83 (±4) | 12.1 | nd[c] | nd[c] | 0.0047 | 2,575 |
| 4 | VIID2[d] | 1188 (±24) | 79 (±2) | 15 | 25.5 (±1.3) | 2,658 (±419) | 0.0096 | 1,563 |

See also Figures S1A and S1B.
[a]The enantiomeric ratio is the ratio of catalytic activity ($k_{cat}/K_M$) with $S_p$-CMP-coumarin to the catalytic activity ($k_{cat}/K_M$) with $R_p$-CMP-coumarin.
[b]Values for rePON1 (G3C9) with $S_p$-CMP coumarin are from (Gupta et al., 2011). Values with $R_p$-CMP-coumarin update previous ones from (Gupta et al., 2011) that were obtained with racemic-CMP-coumarin, using a purified $R_p$- substrate containing $\leq$2% $S_p$-CMP-coumarin.
[c]nd, not detectable.
[d]See Table S1.

blood constituents did not affect their proficiency ex vivo within 24 hr at 37°C.

## Neutralization of VX

Chemical warfare nerve agents are generally divided into G- and V-agents (Romano et al., 2008). Whereas most G-agents have a small and highly reactive fluoride leaving group ($pK_a$ = 3.1), V-type agents have a bulky and far less reactive N,N-dialkylaminoethylthiolate leaving group ($pK_a$ = 7.9) (Bracha and O'Brien, 1968; Figure 1A). V-agents pose a greater threat due to their increased toxicity, persistency, and skin penetration and as such are prime targets for detoxification. However, the hydrolysis of the toxic $S_p$ isomer of VX by wild-type-like rePON1, and by human PON1 (unpublished data), is below the detection limits <2 $M^{-1}$ $min^{-1}$. We found that the previously described GF-detoxifying variants (Gupta et al., 2011) exhibit higher efficiencies with VX, e.g., 80 $M^{-1}$ $min^{-1}$ for 4E9 and 93 $M^{-1}$ $min^{-1}$ for 8C8. Round 4 variants evolved for hydrolyzing GB, GD, and GF were further improved; the catalytic efficiencies of variants VIID2 and VH3 with $S_p$-VX are 132 and 286 $M^{-1}$ $min^{-1}$, respectively. Thus, although these variants were evolved for broad-range G-agent hydrolysis, they also exhibit >100-fold higher rates than wild-type PON1 for VX neutralization.

## DISCUSSION

Our long-term goal is to obtain variants that efficiently detoxify the entire spectrum of G-type nerve agents in vivo. Based on our previously evolved variants for GF detoxification (Gupta et al., 2011), we aimed to increase the hydrolytic activity of PON1 toward the toxic isomers of the three most toxic G-agents, GB (sarin), GD (soman), and GF (cyclosarin), to obtain

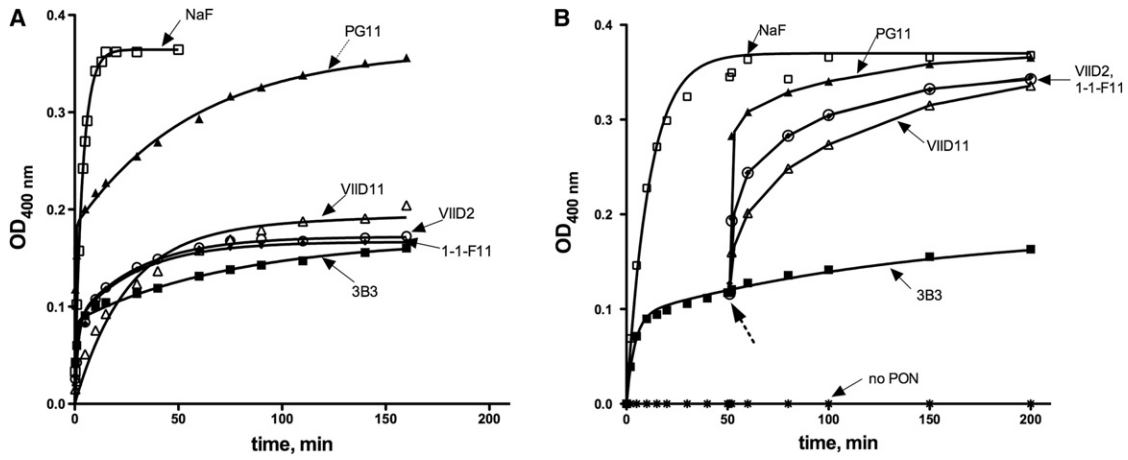


**Figure 3. Hydrolysis of PMP-Coumarin by Evolved Variants**

(A) The hydrolysis of a racemic mixture of PMP-coumarin (10 μM) by various PON1 variants (0.5 μM) was monitored at 400 nm. Complete hydrolysis of all isomers was observed upon addition of NaF (0.25 M). Partial hydrolysis, restricted to $R_p$ isomers ($R_pS_c$, $R_pR_c$), was displayed by the previously described rePON1 variant 3B3 (Ashani et al., 2010).

(B) The hydrolysis of $S_p$ PMP-coumarin isomers ($S_pR_c$,$S_pS_c$) by evolved variants was monitored under similar conditions. Prior to the addition of these variants (indicated by a dashed arrow), samples were pre-incubated with the $R_p$ specific variant 3B3. Complete hydrolysis was monitored by addition of NaF.

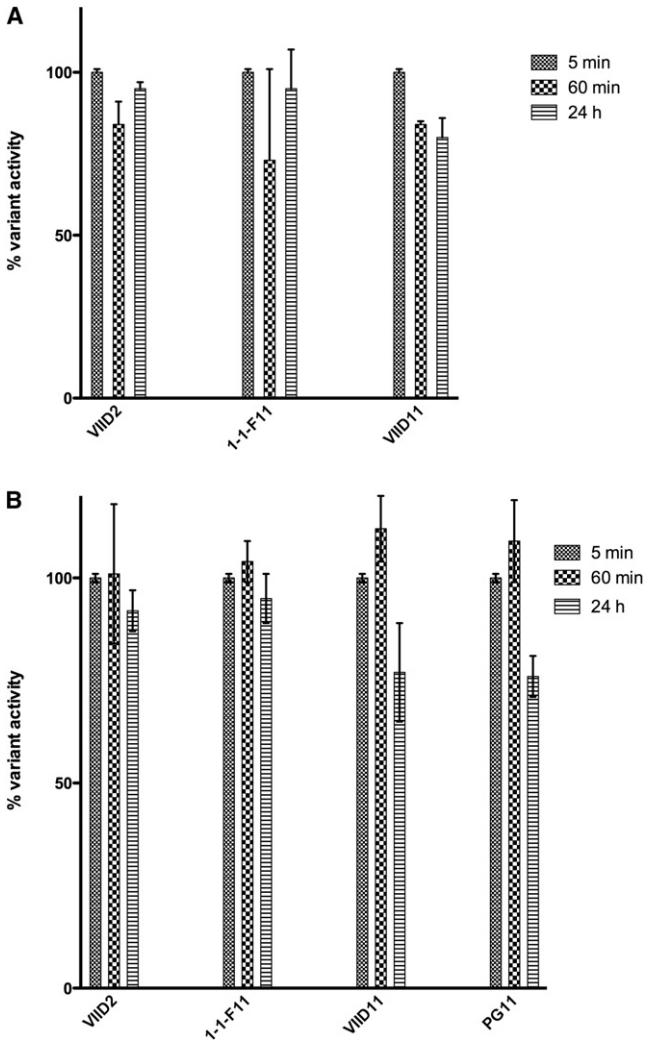


**Figure 4. Activity in Blood Samples**

Error bars represent the standard deviation derived from three independent experiments.

(A) Protection by evolved variants of blood cholinesterases from inhibition by GF. Evolved variants (0.5–2.1 μM) were incubated in whole blood samples (37°C) for 24 hr. GF was added (0.1 μM) and the samples were assayed for residual AChE activity. Cholinesterase protection activity was compared to the initial protection levels observed after 5 min of incubation (41%–45%).

(B) Hydrolytic activity in whole blood samples. Evolved variants (0.3–1.1 μM) were incubated in whole blood samples (37°C) for 24 hr. Incubated samples were diluted in buffer and residual enzyme activities were assayed with CMP-coumarin. The percent activity was determined relative to the hydrolytic activity observed after 5 min incubation.

See also Figure S3.

catalytic efficiency ($k_{cat}/K_M$) values that are $\geq 10^7\ M^{-1}\ min^{-1}$. By selecting variants that exhibit high rates with all three agents, we were able to improve catalytic efficiency while maintaining relatively broad substrate specificity.

Libraries were generated by diversifying the active-site residues of the previously evolved GF-hydrolyzing variant 2D8. The selection pressure was applied gradually by increasing the concentration of the applied G-agents and screening for both GB and GD, as well as GF in one round. The largest improvements were obtained with GD. Owing to the similarity in size and hydrophobicity of their alkyl moieties, the increase in catalytic efficiency toward GD resulted in maintaining or even increasing the activity with GF. However, the improvements in catalytic activity with GB were far more limited. It seems that efficient hydrolysis of GB that contains a smaller moiety (*O*-isopropyl) trades off with efficient hydrolysis of GD and GF that carry bulkier *O*-alkyl groups. Indeed, variants like 5H8, PG11, and VIID2 had improved relative to variants of the previous round with GD or GF at the expense of a reduction in their GB activity (Tables 1 and S1). On the other hand, variants like 2-II-D12 and 1-I-D10 had improved with GB at the expense of their GD or GF activities (Table S1). Thus, beyond a certain threshold of catalytic efficiency, higher catalytic efficiency with the smaller substrate comes at the expense of the bulkier ones. This trend is in accordance with the notion that broad specificity trades off with catalytic efficiency, and that evolutionary "generalists" are less fit than "specialists" in their environments (Straub et al., 2011).

GA fundamentally differs from the three other G-agents in its chemistry (Figure 1A) and its lower in vivo toxicity (Benschop and Dejong, 1988). For these reasons, we did not screen our libraries for GA neutralization. Nonetheless, the evolved variants from rounds 3 and 4 show mild improvements in GA hydrolysis ($\leq$5-fold relative to wild-type-like rePON1). Overall, the activity of improved variants with GA and with GB are ~5-fold lower than our desired goal (Table 1), However, considering GA's and GB's relatively low inhibition constants of AChE (10- to 121-fold lower than that of GD and GF; Benschop and Dejong, 1988; Blum et al., 2008), the catalytic efficiency of round 4 variants might be sufficient to provide effective prophylactic protection against all four G-agents.

Broad specificity and overall improvements in catalytic efficiency were achieved through mutations in positions that are, to our knowledge, new, as well as by the replacement of positions that were already mutated in 2D8 and in other GF evolved variants (Gupta et al., 2011). The re-optimized positions, 69, 115, and 222, had all been shown to increase the activity of PON1 with other OPs (Amitai et al., 2006; Gupta et al., 2011), and their replacement seems to be the key to PON1's "activity maturation" toward various nerve agents. Position 115 is close to PON1's catalytic calcium and mutations in this position trigger a change in PON1's catalytic chemistry. Mutating His115, that takes part in activating the nucleophilic water for lactone hydrolysis, converts PON1 from a lactonase with promiscuous OP hydrolase activity into an OP hydrolase with almost no lactonase activity (Ben-David et al., 2012; Khersonsky and Tawfik, 2006). Position 69 is in contact with 115 and also comprises part of the active-site wall (Harel et al., 2004). Mutations in these two positions seem to be correlated. Under selection for improved GF hydrolysis, the mutation His115Trp was followed by Leu69Gly. The subsequent selection of a G-generalist led to the exchange of Gly69Val in the first round, and of Trp115Ala in the third round (Tables S2 and S6). Concomitant changes in position 222 that faces the opposite side of the catalytic calcium were observed. The mutation Phe222Ser was fixed under selection for GF, and this residue changed again (Ser222Met) under selection for a G-generalist. It therefore seems that PON1's OPH activity is mostly shaped by these three positions.

Other mutated active-site positions include 291 and 332. The Thr332Ser mutation appears to be a global suppressor that accompanies nearly all specificity changes in PON1. The mutation Ile291Leu, in combination with Ser222Met, seems to contribute to the dramatic shift in stereospecificity (e.g., variant 1-I-F11 vs. PG11 Table 3). Leu55Ile (an ancestral mutation in a buried position) probably compensates for the destabilizing effects of active-site mutations, as observed for other ancestral substitutions (Bershtein et al., 2008). Finally, mutations at positions, such as 134 and 136, comprise second-shell mutations because these positions are in contact with mutated active-site positions (e.g., 134 contacts 115).

In addition to highly improved rates, we also observed a dramatic shift in stereoselectivity. This shift is manifested in the enantiomeric ratio of variants with the coumarin analog of GF (Table 3; Figure S1). The E value (ratio of $k_{cat}/K_M$ values) shifted from >1,600-fold in favor of the $R_P$ isomer in wild-type-like rePON1 to >2,500-fold in favor of the $S_P$ isomer of CMP-coumarin in evolved variant 1-I-F11 (Table 3). To our knowledge, a shift in enantiomeric ratio of $>10^6$-fold has not been reported, not even in enzymes that were explicitly evolved for reversal of stereoselectivity (Bartsch et al., 2008; Boersma et al., 2008; Reetz et al., 2001). The screen for protection of AChE led to enzymes that exclusively target the $S_P$ isomers of the applied G-agents. Since the nerve agents are synthesized as racemates, their $R_P$ isomers were also present during screening. However, we observed no inhibition of the $S_P$-CMP-coumarin hydrolyzing activity of the evolved variants by the $R_P$ isomer of CMP-coumarin. Further, the greatest change in stereospecificity occurred in round 3 and was driven by a mild increase (~2- to 3-fold) in the rate of hydrolysis of the $S_P$ isomer and a far larger decrease in the rate of hydrolysis of the $R_P$ isomer ($\leq$52-fold; Table 3). Thus, unlike cases where screening aimed for improved enantioselctivity (Reetz et al., 2009) or even for both higher rates and improved enantioselctivity (Reetz et al., 2010), the drop we observed in hydrolysis rates of the $R_P$ isomer seem to have resulted from the emergence of highly effective $S_P$ hydrolysis (trade-off) and not because of explicit selection for enantioselectivity (for a recent review, see Reetz, 2011).

The stereospecificity of evolved variants also changed with respect to the two toxic carbon isomers of GD ($S_pR_c$ and $S_pS_c$). In the starting point variant 2D8 and in variants of round 1, we detected two phases of hydrolysis with up to 30-fold difference in rate for the two $S_p$-isomers of GD (Tables 1 and S1). This difference disappeared by the end of round 3 as exemplified by variant VIID11 (Figure 2; Table 1). Accordingly, all variants of round 4 exhibited the same rates of hydrolysis of the $S_pR_c$ and $S_pS_c$ isomers. The dramatic gain of stereospecificity toward the toxic $S_P$ isomers, and the loss of specificity with respect to the $S_c/R_c$ GD isomers are both a direct outcome of screening for AChE protection. This screen was designed to reproduce the challenge facing a detoxifying enzyme in vivo, which is to neutralize the nerve agent before it inhibits AChE. The resulting stereselectivities demonstrate the established concept that "you get what you select for" (Romero and Arnold, 2009).

What our in vitro screen does not address is the need for the detoxifying enzyme to be active in human blood and to remain so for extended periods of time. Assuming the administration of a single enzyme dose, the rate of its inactivation and clearance will be mostly determined by processing in organs, such as the liver and kidneys (Katsila et al., 2011; Lin, 2009), by blood components that may inhibit the enzyme, by the overall stability of the enzyme in the blood, and specifically by its susceptibility to proteases in the blood (Patel et al., 2009). The only way to evaluate the combined effect of all these factors is by measuring the residence time of the administered enzyme in vivo. However, this approach is not applicable for screening a large number of variants. We therefore developed a preliminary screen that examines the activity of the PON1 variants in human blood ex vivo (Ashani et al., 2011). According to this preliminary test, the broad spectrum variants described here appear to maintain ChE protection in blood at levels that are comparable to buffer, and maintain $\geq$75% activity for at least 24 hr at 37°C.

Finally, the dramatic improvement of evolved variants with G-agents prompted us to examine their ability to hydrolyze VX. In contrast to wild-type PON1, the evolved variants described here show measurable rates ($k_{cat}/K_M$ values of 132 to 286 $M^{-1}$ $min^{-1}$) with the toxic isomer of VX. Most crucially, this activity is sufficiently high to be assayed for VX neutralization using crude bacterial lysates, thus opening the road for screening libraries and for evolving PON1 toward efficient V-agent hydrolysis.

## SIGNIFICANCE

**We describe the enzyme variants that hydrolyze the toxic isomers of G-type nerve agents with sufficiently high rates to detoxify these agents in vivo, such that prophylactic protection could be potentially achieved upon administering low enzyme doses. Following only four rounds of directed evolution, we obtained variants that were improved up to 340-fold relative to our previously described GF-hydrolyzing variant. Overall, these variants show 40- to 3,400-fold higher catalytic efficiencies than wild-type PON1 for hydrolyzing the toxic isomers of the three most toxic G-agents (GB, GD, and GF). Their $k_{cat}/K_M$ values for GD and GF neutralization are particularly high: 3-5 $\times$ $10^7$ $M^{-1}$ $min^{-1}$. Although lower by about an order of magnitude, their catalytic efficiencies with GA and GB may still enable effective prophylaxis because of the lower toxicity of these agents. This work, therefore, demonstrates that, despite tradeoffs between different substrates, catalytically efficient broad-spectrum, generalist enzymes can evolve. Although the evolved variants show relatively broad specificity with respect to the substrate's O-alkyl group, their stereospecificity is remarkably high. Screening for variants that hydrolyze the toxic $S_p$ isomers resulted in possibly the highest recorded shift in enantiomeric preference between the wild-type enzyme and its evolved variants ($E^{evolved}/E^{wild\text{-}type} > 10^6$). Overall, this work describes promising candidates for in vivo tests of prophylaxis and postexposure treatment and a general scheme for the evolution of highly active OP hydrolyzing enzymes that could detoxify a broad range of nerve agents and pesticides. It demonstrates the powers of laboratory evolution and its ability to completely reshape the catalytic activity and substrate specificity, as well as the stereoselectivity of enzymes.**

 

## EXPERIMENTAL PROCEDURES

### Gene Libraries

Recombinant PON1 variants cloned into a pET vector with a C-terminal 6-His tag (Gupta et al., 2011) were used as the template for library construction using synthetic oligonucleotides and the ISOR protocol (Herman and Tawfik, 2007). Briefly, the genes of PON1 variants were PCR amplified, treated with *Dpn*I (NEB) and purified. Purified DNA (20 μg in 150 μl) was digested with 0.3 U *DNase*I (Takara, Tokyo, Japan) at 37°C for 0.5, 1, 1.5 and 2 min. The reactions were terminated with 16 μl of 0.5 M ethylenediaminetetraacetic acid (EDTA), inactivated at 80°C for 15 min, and run on 2% agarose gel. Fragments of 50–150 bps size were excised and purified by a gel extraction (Qiagen, Venlo, The Netherlands). The intact gene was reassembled by PCR from the DNA fragments (100 ng) with the addition of synthetic oligonucleotides (1-10 nM; Table S9). The assembly product was amplified by nested PCR using primers pET-Nes1-Bc and pET-Nes0-Fo (Gupta et al., 2011), purified, digested, (*Nco*I, *Not*I), and recloned into the pET32 vector.

### Screening

BL21/DE3 cells expressing PON1 variants were plated on LB-agar plates (plus 100 mg/l ampicillin and 1% glucose) and grown O/N at 37°C. Randomly picked colonies were individually grown in 96-deep-wells plates (500 μl 2YT per well, plus ampicillin and $CaCl_2$ 1mM) for 24 hr at R.T. Cells were pelleted, frozen (−80°C, 20 min), resuspended (200 μl, 0.1M Tris-HCl [pH 8.0], 1mM $CaCl_2$, 10 μg/ml lysozyme, 0.2% Triton X-100, and 5 units/ml benzonase; Novagen, Madison, WI, USA), lysed (1300 rpm, 45 min, 37°C) and centrifuged (4000 rpm, 20 min, 4°C). Clarified cell lysates (40 μl) were mixed with an AChE solution (40 μl, 1nM reAChE [Gupta et al., 2011], in phosphate buffered saline [PBS], 0.1% BSA) in 96 well plates using an automated liquid-handling system (Precision 2000, BioTek, Winooski, VT, USA). In situ generated G-agents (Gupta et al., 2011; 20 μl, 0.1–1.5 μM) were added. Following 30 min incubation, reaction samples (20 μl) were mixed with the AChE substrate and DTNB (180 μl, 0.85 mM DTNB, and 0.55 mM acetylthiocholine in PBS) and initial rates were measured at 412 nm. The percentage of residual AChE activity was determined.

### Enzymes Purification

Cultures of BL21/DE3 plasmid transformed cells were grown ($OD_{600nm}$ = 0.5, 37°C), induced (IPTG 1 mM, 4 h), harvested, resuspended, and disrupted by sonication. Ammonium sulfate was added (55% w/v). The precipitate was dissolved and dialyzed against activity buffer (Tris-HCl 50 mM [pH 8], $CaCl_2$ 1mM, NaCl 50mM, and Tergitol 0.1%) and purified on Ni-NTA (Novagen). Fractions were analyzed for purity (by SDS-PAGE), pooled, dialyzed against activity buffer supplemented with 0.02% sodium azide, and stored at 4°C. Protein purity was typically 70%–85% by SDS-PAGE gel.

### Determination of $k_{cat}/K_M$ by AChE Inhibition

In situ generated agents (40 nM; Gupta et al., 2011) were mixed with purified PON1 variants (10-0.01 μM) in activity buffer. Reaction mixture samples were diluted (1:10) into an AChE solution (4 nM TcAChE, 0.1% BSA, and 1 mM EDTA in PBS), incubated 15 min), and their residual AChE activity was determined as described above. The %-inhibition of AChE by the G-agent without preincubation with a PON variant was considered as 100% inhibition. Normalized %-inhibition values were calculated, and the apparent $k_{cat}/K_M$ was derived from the slope of the resulting single exponential curve.

### Determination of $k_{cat}/K_M$ Values with $S_p/R_p$-CMP-Coumarin

$S_p$-CMP-coumarin was obtained by digestion of racemic CMP-coumarin with variant 3B3 that is $R_p$-CMP-coumarin specific (Ashani et al., 2010), followed by organic extraction of the intact. $S_p$-CMP-coumarin. $R_p$-CMP-coumarin was obtained in a similar manner using variant VIID2 that is $S_p$-CMP-coumarin specific. Purified variants (0.01–0.6 μM) were mixed with either $S_p$ or $R_p$-CMP-coumarin (5-1000 μM) in activity buffer in 96-well enzyme-linked immunosorbent assay plates (200 μl per reaction). Product formation was monitored for 5 min at 405 nm and initial velocities were derived. Values of at least three independent repeats were averaged for determining the kinetic parameters of each variant by fitting the data directly to a Michaelis-Menten equation using KaleidaGraph. Substrate concentrations were verified by monitoring their complete hydrolysis using NaF (100 mM).

### Kinetic Assay with PMP-Coumarin

Purified variants (0.5 μM) were mixed with racemic PMP-coumarin (10 μM) and activity buffer as above. The rate of PMP-coumarin hydrolysis was monitored by measuring the absorbance of released coumarin at 405 nm for up to 200 min. Alternatively, purified $R_p$-specific variant 3B3 (Ashani et al., 2010; 0.5 μM) was mixed with racemic PMP-coumarin (10 μM) and activity buffer and product release was monitored for 50 min. Then, the evolved variants were added (0.5 μM) and product release was monitored for additional 150 min.

### Kinetics of GA Hydrolysis by $^{31}P$ NMR

GA was synthesized at a small (mg) scale without distillation using a modified protocol (1951, Acta Physiol. Scand. Suppl. 90, 25) and purified of a silica gel column. A Varian 300 MHz was used to monitor the changes in the $^{31}P$ NMR signal of reaction mixtures of GA with PON1 variants. In an NMR tube, 0.15 ml $D_2O$ were added to 0.3 ml reactivity buffer containing 1 mg O,O-diisopropyl methylphosphonate and the solution was spiked with 50 μl of a GA stock solution in aceton to provide a final concentration of 1 mg/ml. After recording the baseline spectrum, the reaction was initiated by the addition of the corresponding PON1 variant. Twenty pulses were collected for each scan, data acquisition was repeated every 2-3 min.

### Ex Vivo Assays

Protection of ChE's in human whole blood samples was measured as described (Ashani et al., 2011). Briefly, purified PON1 variants (0.3–2.5 μM) were added to pre-heated (37°C) human whole blood samples (obtained from the Israeli blood bank), spiked with $CaCl_2$ (to 2 mM) and adjusted to pH 7.4 with Tris base (1 M). At selected time intervals, in situ prepared GF was added (0.1 μM) and the residual activity of blood ChEs was assayed as described (Ashani et al., 2011). The ChE activity was compared to the residual ChEs activity obtained after 5 min incubation in blood. The hydrolytic activity of PON1 variants (0.3–2.5 μM) following incubation in whole blood (pH 7.4, $CaCl_2$ 2mM) was evaluated by dilution of PON1 containing blood samples (1,000-fold) at different time intervals into activity buffer, addition of racemic CMP-coumarin (0.3 mM), and measurement of the rate of hydrolysis as above. These rates were compared to the rates obtained after 5 min incubation.

## SUPPLEMENTAL INFORMATION

Supplemental Information includes five figures and nine tables and can be found with this article online at doi:10.1016/j.chembiol.2012.01.017.

## ACKNOWLEDGMENTS

Financial support is gratefully acknowledged by the Defense Threat Reduction Agency (DTRA) of the US Department of Defense (contract HDTRA1-07-C−0024), the CounterACT Program, National Institutes Of Health Office of the Director, and the National Institute of Neurological Diseases and Stroke (grant number U54-NS058183), as well as by grants from the Willner Albert and Blanche foundation and Jack Wolgin. The authors declare that a patent application regarding the described variants has been filed by the Weizmann Institute of Science. Author contributions: M.G. designed the experiments, constructed and screened libraries, isolated and characterized variants, analyzed data and wrote the paper. Y.A. synthesized substrates, characterized variants, designed and performed ex-vivo experiments and contributed to writing the paper. Y.S. screened variant libraries. M.B.-D. assisted library design. H.L. synthesized substrates and performed $^{31}P$ NMR experiments. I.S. contributed to editing the paper. J.L.S. performed structural analysis and contributed to editing the paper. D.S.T. designed the experiments, analyzed data and wrote the paper.

Received: December 13, 2011
Revised: January 16, 2012
Accepted: January 18, 2012
Published: April 19, 2012

## REFERENCES

Aharoni, A., Gaidukov, L., Yagur, S., Toker, L., Silman, I., and Tawfik, D.S. (2004). Directed evolution of mammalian paraoxonases PON1 and PON3 for bacterial expression and catalytic specialization. Proc. Natl. Acad. Sci. USA *101*, 482–487.

Alcolombri, U., Elias, M., and Tawfik, D.S. (2011). Directed evolution of sulfotransferases and paraoxonases by ancestral libraries. J. Mol. Biol. *411*, 837–853.

Amitai, G., Gaidukov, L., Adani, R., Yishay, S., Yacov, G., Kushnir, M., Teitlboim, S., Lindenbaum, M., Bel, P., Khersonsky, O., et al. (2006). Enhanced stereoselective hydrolysis of toxic organophosphates by directly evolved variants of mammalian serum paraoxonase. FEBS J. *273*, 1906–1919.

Ashani, Y., Gupta, R.D., Goldsmith, M., Silman, I., Sussman, J.L., Tawfik, D.S., and Leader, H. (2010). Stereo-specific synthesis of analogs of nerve agents and their utilization for selection and characterization of paraoxonase (PON1) catalytic scavengers. Chem. Biol. Interact. *187*, 362–369.

Ashani, Y., Goldsmith, M., Leader, H., Silman, I., Sussman, J.L., and Tawfik, D.S. (2011). In vitro detoxification of cyclosarin in human blood pre-incubated ex vivo with recombinant serum paraoxonases. Toxicol. Lett. *206*, 24–28.

Bartsch, S., Kourist, R., and Bornscheuer, U.T. (2008). Complete inversion of enantioselectivity towards acetylated tertiary alcohols by a double mutant of a Bacillus subtilis esterase. Angew. Chem. Int. Ed. Engl. *47*, 1508–1511.

Ben-David, M., Elias, M., Filippi, J.-J., Duñach, E., Silman, I., Sussman, J.L., and Tawfik, D.S. (2012). Catalytic versatility and backups in enzyme active-sites: the case of serum paraoxonase 1. J. Mol. Biol. *418*, 181–196.

Benschop, H.P., Konings, C.A., Van Genderen, J., and De Jong, L.P. (1984). Isolation, anticholinesterase properties, and acute toxicity in mice of the four stereoisomers of the nerve agent soman. Toxicol. Appl. Pharmacol. *72*, 61–74.

Benschop, H.P., and Dejong, L.P.A. (1988). Nerve agent stereoisomers - analysis, isolation, and toxicology. Acc. Chem. Res. *21*, 368–374.

Bershtein, S., Goldin, K., and Tawfik, D.S. (2008). Intense neutral drifts yield robust and evolvable consensus proteins. J. Mol. Biol. *379*, 1029–1044.

Blum, M.M., Timperley, C.M., Williams, G.R., Thiermann, H., and Worek, F. (2008). Inhibitory potency against human acetylcholinesterase and enzymatic hydrolysis of fluorogenic nerve agent mimics by human paraoxonase 1 and squid diisopropyl fluorophosphatase. Biochemistry *47*, 5216–5224.

Boersma, Y.L., Pijning, T., Bosma, M.S., van der Sloot, A.M., Godinho, L.F., Dröge, M.J., Winter, R.T., van Pouderoyen, G., Dijkstra, B.W., and Quax, W.J. (2008). Loop grafting of Bacillus subtilis lipase A: inversion of enantioselectivity. Chem. Biol. *15*, 782–789.

Bracha, P., and O'Brien, R.D. (1968). Trialkyl phosphate and phosphorothiolate anticholinesterases. I. Amiton analogs. Biochemistry *7*, 1545–1554.

Cannard, K. (2006). The acute treatment of nerve agent exposure. J. Neurol. Sci. *249*, 86–94.

Carletti, E., Colletier, J.P., Dupeux, F., Trovaslet, M., Masson, P., and Nachon, F. (2010). Structural evidence that human acetylcholinesterase inhibited by tabun ages through O-dealkylation. J. Med. Chem. *53*, 4002–4008.

Chen, F., Gaucher, E.A., Leal, N.A., Hutter, D., Havemann, S.A., Govindarajan, S., Ortlund, E.A., and Benner, S.A. (2010). Reconstructed evolutionary adaptive paths give polymerases accepting reversible terminators for sequencing and SNP detection. Proc. Natl. Acad. Sci. USA *107*, 1948–1953.

diTargiani, R.C., Chandrasekaran, L., Belinskaya, T., and Saxena, A. (2010). In search of a catalytic bioscavenger for the prophylaxis of nerve agent toxicity. Chem. Biol. Interact. *187*, 349–354.

Doctor, B.P., and Saxena, A. (2005). Bioscavengers for the protection of humans against organophosphate toxicity. Chem. Biol. Interact. *157-158*, 167–171.

Draganov, D.I. (2010). Lactonases with organophosphatase activity: structural and evolutionary perspectives. Chem. Biol. Interact. *187*, 370–372.

Dunn, M.A., and Sidell, F.R. (1989). Progress in medical defense against nerve agents. JAMA *262*, 649–652.

Gupta, R.D., Goldsmith, M., Ashani, Y., Simo, Y., Mullokandov, G., Bar, H., Ben-David, M., Leader, H., Margalit, R., Silman, I., et al. (2011). Directed evolution of hydrolases for prevention of G-type nerve agent intoxication. Nat. Chem. Biol. *7*, 120–125.

Harel, M., Aharoni, A., Gaidukov, L., Brumshtein, B., Khersonsky, O., Meged, R., Dvir, H., Ravelli, R.B., McCarthy, A., Toker, L., et al. (2004). Structure and evolution of the serum paraoxonase family of detoxifying and anti-atherosclerotic enzymes. Nat. Struct. Mol. Biol. *11*, 412–419.

Hemmert, A.C., Otto, T.C., Chica, R.A., Wierdl, M., Edwards, J.S., Lewis, S.L., Edwards, C.C., Tsurkan, L., Cadieux, C.L., Kasten, S.A., et al. (2011). Nerve agent hydrolysis activity designed into a human drug metabolism enzyme. PLoS ONE *6*, e17441.

Herman, A., and Tawfik, D.S. (2007). Incorporating synthetic oligonucleotides via gene reassembly (ISOR): a versatile tool for generating targeted libraries. Protein Eng. Des. Sel. *20*, 219–226.

Katsila, T., Siskos, A.P., and Tamvakopoulos, C. (2011). Peptide and protein drugs: the study of their metabolism and catabolism by mass spectrometry. Mass Spectrom. Rev. *31*, 110–133.

Khersonsky, O., and Tawfik, D.S. (2005). Structure-reactivity studies of serum paraoxonase PON1 suggest that its native activity is lactonase. Biochemistry *44*, 6371–6382.

Khersonsky, O., and Tawfik, D.S. (2006). The histidine 115-histidine 134 dyad mediates the lactonase activity of mammalian serum paraoxonases. J. Biol. Chem. *281*, 7649–7656.

Lenz, D.E., Yeung, D., Smith, J.R., Sweeney, R.E., Lumley, L.A., and Cerasoli, D.M. (2007). Stoichiometric and catalytic scavengers as protection against nerve agent toxicity: a mini review. Toxicology *233*, 31–39.

Lin, J.H. (2009). Pharmacokinetics of biotech drugs: peptides, proteins and monoclonal antibodies. Curr. Drug Metab. *10*, 661–691.

Newmark, J. (2007). Nerve agents. Neurologist *13*, 20–32.

Patel, N., Krishnan, S., Offman, M.N., Krol, M., Moss, C.X., Leighton, C., van Delft, F.W., Holland, M., Liu, J., Alexander, S., et al. (2009). A dyad of lymphoblastic lysosomal cysteine proteases degrades the antileukemic drug L-asparaginase. J. Clin. Invest. *119*, 1964–1973.

Reetz, M.T., Wilensek, S., Zha, D., and Jaeger, K.E. (2001). Directed evolution of an enantioselective enzyme through combinatorial multiple-cassette mutagenesis. Angew. Chem. Int. Ed. Engl. *40*, 3589–3591.

Reetz, M.T. (2011). Laboratory evolution of stereoselective enzymes: a prolific source of catalysts for asymmetric reactions. Angew. Chem. Int. Ed. Engl. *50*, 138–174.

Reetz, M.T., Bocola, M., Wang, L.W., Sanchis, J., Cronin, A., Arand, M., Zou, J., Archelas, A., Bottalla, A.L., Naworyta, A., and Mowbray, S.L. (2009). Directed evolution of an enantioselective epoxide hydrolase: uncovering the source of enantioselectivity at each evolutionary stage. J. Am. Chem. Soc. *131*, 7334–7343.

Reetz, M.T., Prasad, S., Carballeira, J.D., Gumulya, Y., and Bocola, M. (2010). Iterative saturation mutagenesis accelerates laboratory evolution of enzyme stereoselectivity: rigorous comparison with traditional methods. J. Am. Chem. Soc. *132*, 9144–9152.

Romano, J.A., Lukey, B.J., and Salem, H. (2008). Chemical Warfare Agents: Chemistry, Pharmacology, Toxicology, and Therapeutics (Boca Raton: CRC Press).

Romero, P.A., and Arnold, F.H. (2009). Exploring protein fitness landscapes by directed evolution. Nat. Rev. Mol. Cell Biol. *10*, 866–876.

Seo, D., and Goldschmidt-Clermont, P. (2009). The paraoxonase gene family and atherosclerosis. Curr. Atheroscler. Rep. *11*, 182–187.

Straub, C.S., Ives, A.R., and Gratton, C. (2011). Evidence for a trade-off between host-range breadth and host-use efficiency in aphid parasitoids. Am. Nat. *177*, 389–395.

Theriot, C.M., and Grunden, A.M. (2011). Hydrolysis of organophosphorus compounds by microbial enzymes. Appl. Microbiol. Biotechnol. *89*, 35–43.

Tsai, P.C., Bigley, A., Li, Y., Ghanem, E., Cadieux, C.L., Kasten, S.A., Reeves, T.E., Cerasoli, D.M., and Raushel, F.M. (2010). Stereoselective hydrolysis of organophosphate nerve agents by the bacterial phosphotriesterase. Biochemistry *49*, 7978–7987.

 